

Evolution from BCS to BEC superfluidity in the presence of spin-orbit coupling

Li Han and C. A. R. Sá de Melo

School of Physics, Georgia Institute of Technology, Atlanta, Georgia 30332, USA

(Dated: August 15, 2018)

We discuss the evolution from BCS to BEC superfluids in the presence of spin-orbit coupling, and show that this evolution is just a crossover in the balanced case. The dependence of several thermodynamic properties, such as the chemical potential, order parameter, pressure, entropy, isothermal compressibility and spin susceptibility tensor on the spin-orbit coupling and interaction parameter at low temperatures are analyzed. We studied both the case of equal Rashba and Dresselhaus (ERD) and the Rashba-only (RO) spin-orbit coupling. Comparisons between the two cases reveal several striking differences in the corresponding thermodynamic quantities. Finally we propose measuring the spin susceptibility as a means to detect the spin-orbit coupling effect.

PACS numbers: 03.75.Ss, 67.85.Lm, 67.85.-d

Superfluidity is a ubiquitous phenomenon that is encountered in nearly every area of physics including condensed matter, nuclear, astro, and atomic and molecular physics. Superflow results from strong correlations between particles, which for any given interacting Fermi system could not be controlled externally until recently with the advent of ultra-cold atoms. In standard condensed matter there is a continuous search for new charged superfluids (superconductors) since the type and strength of interactions can not be tuned even within the same class of materials. In the case of nuclear matter the issue of tunability of interactions is even worse, being hopeless for neutron stars. However, the situation is much more favorable for ultra-cold Fermi atoms, where the ability to control interactions between particles, via Feshbach resonances, has been demonstrated in experimental studies of the so-called crossover from BCS to BEC superfluidity.

Further control of interactions is now possible through newly developed experimental techniques that allow the production of fictitious magnetic fields which couple to neutral bosonic atoms [1, 2]. These fictitious magnetic fields are generated through an all optical process, but produce real effects like the creation of vortices in the superfluid state of bosons. Furthermore, artificial spin-orbit coupling has also been produced in neutral bosonic systems [3] where the strength of the coupling can be controlled optically. In principle the same techniques can be applied to ultracold fermions [3, 4], which, when coupled with the control over the interaction using Feshbach resonances, allows for the exploration of superfluidity not only as a function of interactions, but also as a function of fictitious magnetic fields [5], or as a function of spin-orbit coupling discussed here. An introduction to the effects of controllable fictitious magnetic and spin-orbit fields can now be found in the literature [6].

It is in anticipation of experiments involving spin-orbit coupling in fermionic atoms such as ^6Li , ^{40}K and isotopes of Ytterbium, that we discuss here the evolution from BCS to BEC superfluidity in the presence of controllable

spin-orbit couplings for balanced fermions in three dimensions. We investigate spin-orbit effects with Dresselhaus [7] and/or Rashba [8] terms, and analyze several thermodynamic quantities including the order parameter, chemical potential, thermodynamic potential, entropy, pressure, isothermal compressibility, and spin susceptibility tensor as a function of spin-orbit coupling and interaction parameter at low temperatures. We conclude that the BCS-to-BEC evolution for balanced fermions including spin-orbit effects is just a crossover.

Hamiltonian: To address the problem of the evolution from BCS to BEC superfluidity in the presence of spin-orbit fields for balanced or imbalanced Fermi-Fermi mixtures, we start with the generic Hamiltonian density

$$\mathcal{H}(\mathbf{r}) = \mathcal{H}_0(\mathbf{r}) + \mathcal{H}_I(\mathbf{r}). \quad (1)$$

The single-particle Hamiltonian density is

$$\mathcal{H}_0(\mathbf{r}) = \sum_{\alpha\beta} \psi_{\alpha}^{\dagger}(\mathbf{r}) \left[\hat{K}_{\alpha} \delta_{\alpha\beta} - h_i(\mathbf{r}) \sigma_{i,\alpha\beta} \right] \psi_{\beta}(\mathbf{r}), \quad (2)$$

where $\hat{K}_{\alpha} = -\nabla^2/(2m_{\alpha}) - \mu_{\alpha}$ is the kinetic energy in reference to the chemical potential μ_{α} , and $h_i(\mathbf{r})$ is the spin-orbit field along the i -direction ($\alpha = \uparrow, \downarrow$, $i = x, y, z$). The interaction term is $\mathcal{H}_I(\mathbf{r}) = -g\psi_{\uparrow}^{\dagger}(\mathbf{r})\psi_{\downarrow}^{\dagger}(\mathbf{r})\psi_{\downarrow}(\mathbf{r})\psi_{\uparrow}(\mathbf{r})$, where g is a contact interaction. In this paper we set $\hbar = k_B = 1$.

Effective Action: The partition function at temperature T is $Z = \int \mathcal{D}[\psi, \psi^{\dagger}] \exp(-S[\psi, \psi^{\dagger}])$ with action

$$S[\psi, \psi^{\dagger}] = \int d\tau d\mathbf{r} \left[\sum_{\alpha} \psi_{\alpha}^{\dagger}(\mathbf{r}) \frac{\partial}{\partial \tau} \psi_{\alpha}(\mathbf{r}) + \mathcal{H}(\mathbf{r}, \tau) \right]. \quad (3)$$

Using the standard Hubbard-Stratanovich transformation that introduces the pairing field $\Delta(\mathbf{r}, \tau) = g\langle \psi_{\downarrow}(\mathbf{r}, \tau)\psi_{\uparrow}(\mathbf{r}, \tau) \rangle$ we can write the intermediate action $S_{\text{int}}[\psi, \psi^{\dagger}, \Delta, \Delta^{\dagger}] = S_{\text{no}}[\psi, \psi^{\dagger}] + S_I[\psi, \psi^{\dagger}, \Delta, \Delta^{\dagger}]$, where the no-interaction action is

$$S_{\text{no}}[\psi, \psi^{\dagger}] = \int d\tau d\mathbf{r} \left[\sum_{\alpha} \psi_{\alpha}^{\dagger}(\mathbf{r}) \frac{\partial}{\partial \tau} \psi_{\alpha}(\mathbf{r}) + \mathcal{H}_0(\mathbf{r}, \tau) \right],$$

and the action due to the auxiliary field is

$$S_I = \int d\tau d\mathbf{r} \left[\frac{|\Delta(\mathbf{r}, \tau)|^2}{g} - \Delta \psi_\uparrow^\dagger \psi_\downarrow^\dagger - \Delta^\dagger \psi_\downarrow \psi_\uparrow \right].$$

Using the four-dimensional vector $\Psi^\dagger = \{\psi_\uparrow^\dagger, \psi_\downarrow^\dagger, \psi_\uparrow, \psi_\downarrow\}$, the intermediate action becomes

$$S_{\text{int}} = \int d\tau d\mathbf{r} \left[\frac{|\Delta(\mathbf{r}, \tau)|^2}{g} + \frac{1}{2} \Psi^\dagger \mathbf{M} \Psi + \frac{1}{2} (\tilde{K}_\uparrow + \tilde{K}_\downarrow) \right].$$

The 4×4 matrix \mathbf{M} is

$$\mathbf{M} = \begin{pmatrix} \partial_\tau + \tilde{K}_\uparrow & -h_\perp & 0 & -\Delta \\ -h_\perp^* & \partial_\tau + \tilde{K}_\downarrow & \Delta & 0 \\ 0 & \Delta^\dagger & \partial_\tau - \tilde{K}_\uparrow & h_\perp^* \\ -\Delta^\dagger & 0 & h_\perp & \partial_\tau - \tilde{K}_\downarrow \end{pmatrix}, \quad (4)$$

where $h_\perp = h_x - ih_y$ corresponds to the transverse component of the spin-orbit field, h_z to the parallel component with respect to the quantization axis z , $\tilde{K}_\uparrow = \hat{K}_\uparrow - h_z$, and $\tilde{K}_\downarrow = \hat{K}_\downarrow + h_z$. Integration over the fields Ψ and Ψ^\dagger leads to the effective action

$$S_{\text{eff}} = \int d\tau d\mathbf{r} \left[\frac{|\Delta(\mathbf{r}, \tau)|^2}{g} - \frac{T}{2V} \ln \det \frac{\mathbf{M}}{T} + \tilde{K}_+ \delta(\mathbf{r} - \mathbf{r}') \right], \quad (5)$$

where $\tilde{K}_+ = (\tilde{K}_\uparrow + \tilde{K}_\downarrow)/2$.

Saddle Point Approximation: To proceed we use the saddle point approximation $\Delta(\mathbf{r}, \tau) = \Delta_0 + \eta(\mathbf{r}, \tau)$, and separate the matrix \mathbf{M} into two parts. The first one is the saddle point matrix \mathbf{M}_0 , where the transformation $\Delta(\mathbf{r}, \tau) \rightarrow \Delta_0$ takes $\mathbf{M} \rightarrow \mathbf{M}_0$. The second one is the fluctuation matrix $\mathbf{M}_F = \mathbf{M} - \mathbf{M}_0$, which depends only on $\eta(\mathbf{r}, \tau)$ and its Hermitian conjugate.

Using the saddle point approach we write the effective action as $S_{\text{eff}} = S_0 + S_F$, where

$$S_0 = \int d\tau d\mathbf{r} \left[\frac{|\Delta_0|^2}{g} - \frac{T}{2V} \ln \det \frac{\mathbf{M}_0}{T} + \tilde{K}_+ \delta(\mathbf{r} - \mathbf{r}') \right]$$

is the saddle point action and

$$S_F = \int d\tau d\mathbf{r} \left[\frac{|\eta(\mathbf{r}, \tau)|^2}{g} - \frac{T}{2V} \ln \det (\mathbf{1} + \mathbf{M}_0^{-1} \mathbf{M}_F) \right]$$

is the fluctuation action in all orders in the fluctuation field. The effects of fluctuations at both zero temperature and near the critical temperature will be discussed later.

A transformation to the momentum-frequency coordinates $(\mathbf{k}, i\omega_n)$, where $\omega_n = (2n + 1)\pi T$, leads to

$$S_0 = \frac{V}{T} \frac{|\Delta_0|^2}{g} - \frac{1}{2} \sum_{k, i\omega_n, j} \ln \left[\frac{i\omega_n - E_j(\mathbf{k})}{T} \right] + \sum_{\mathbf{k}} \frac{\tilde{K}_+}{T},$$

where $E_j(\mathbf{k})$ are the eigenvalues of the matrix

$$\mathbf{H}_0 = \begin{pmatrix} \tilde{K}_\uparrow(\mathbf{k}) & -h_\perp(\mathbf{k}) & 0 & -\Delta_0 \\ -h_\perp^*(\mathbf{k}) & \tilde{K}_\downarrow(\mathbf{k}) & \Delta_0 & 0 \\ 0 & \Delta_0^\dagger & -\tilde{K}_\uparrow(-\mathbf{k}) & h_\perp^*(-\mathbf{k}) \\ -\Delta_0^\dagger & 0 & h_\perp(-\mathbf{k}) & -\tilde{K}_\downarrow(-\mathbf{k}) \end{pmatrix}, \quad (6)$$

which describes the Hamiltonian of the elementary excitations in the four-dimensional vector basis $\Psi^\dagger = \{\psi_\uparrow^\dagger(\mathbf{k}), \psi_\downarrow^\dagger(\mathbf{k}), \psi_\uparrow(-\mathbf{k}), \psi_\downarrow(-\mathbf{k})\}$. The spin-orbit field is $\mathbf{h}_\perp(\mathbf{k}) = \mathbf{h}_R(\mathbf{k}) + \mathbf{h}_D(\mathbf{k})$, where the first term is of the Rashba-type $\mathbf{h}_R(\mathbf{k}) = v_R(-k_y \hat{\mathbf{x}} + k_x \hat{\mathbf{y}})$, and the second is of the Dresselhaus-type $\mathbf{h}_D(\mathbf{k}) = v_D(k_y \hat{\mathbf{x}} + k_x \hat{\mathbf{y}})$. We assume, without loss of generality, that $v_R > 0$ and $v_D > 0$. The magnitude of the transverse field is then $h_\perp(\mathbf{k}) = \sqrt{(v_D - v_R)^2 k_y^2 + (v_D + v_R)^2 k_x^2}$. In the limiting cases of pure Rashba (R) with $v_D = 0$ and for equal Rashba-Dresselhaus (ERD) couplings with $v_R = v_D = v/2$, the transverse fields are $h_\perp(\mathbf{k}) = v_R \sqrt{k_x^2 + k_y^2}$ ($v_R > 0$) and $h_\perp(\mathbf{k}) = v|k_x|$ ($v > 0$), respectively.

Order parameter and number equations: The saddle point thermodynamic potential $\Omega_0 = TS_0$ is obtained by integrating out the fermions leading to

$$\Omega_0 = V \frac{|\Delta_0|^2}{g} - \frac{T}{2} \sum_{\mathbf{k}, j} \ln \{1 + \exp[-E_j(\mathbf{k})/T]\} + \sum_{\mathbf{k}} \tilde{K}_+,$$

with $\tilde{K}_+ = [\tilde{K}_\uparrow(-\mathbf{k}) + \tilde{K}_\downarrow(-\mathbf{k})]/2$. The order parameter is determined via the minimization of Ω_0 with respect to $|\Delta_0|^2$ leading to

$$\frac{V}{g} = -\frac{1}{2} \sum_{\mathbf{k}, j} n_F [E_j(\mathbf{k})] \frac{\partial E_j(\mathbf{k})}{\partial |\Delta_0|^2}, \quad (7)$$

where $n_F [E_j(\mathbf{k})] = 1/(\exp[E_j(\mathbf{k})/T] + 1)$ is the Fermi function for energy $E_j(\mathbf{k})$. We replace the contact interaction g by the scattering length a_s through the relation $1/g = -m_+/(4\pi a_s) + (1/V) \sum_{\mathbf{k}} [1/(2\epsilon_{\mathbf{k},+})]$, where $m_+ = 2m_\downarrow m_\uparrow / (m_\downarrow + m_\uparrow)$ is twice of the reduced mass, $\epsilon_{\mathbf{k},\alpha} = k^2/(2m_\alpha)$ are the kinetic energies, and $\epsilon_{\mathbf{k},+} = [\epsilon_{\mathbf{k},\uparrow} + \epsilon_{\mathbf{k},\downarrow}]/2$. The number of particles at the saddle point is obtained by $N_\alpha = -\partial \Omega_0 / \partial \mu_\alpha$, leading to

$$N_\alpha = \frac{1}{2} \sum_{\mathbf{k}} \left[1 - \sum_j n_F [E_j(\mathbf{k})] \frac{\partial E_j(\mathbf{k})}{\partial \mu_\alpha} \right]. \quad (8)$$

The self-consistent relations shown in Eqs. (7) and (8) are general for arbitrary mass and population imbalances. However, next, we particularize our discussion to the case of a balanced system with equal masses.

Balanced Populations: In the case of mass and population balanced systems, the four eigenvalues of the matrix \mathbf{H}_0 are $E_1(\mathbf{k}) = \sqrt{[\epsilon_1(\mathbf{k})]^2 + |\Delta_0|^2}$, $E_2(\mathbf{k}) = \sqrt{[\epsilon_2(\mathbf{k})]^2 + |\Delta_0|^2}$, $E_3(\mathbf{k}) = -E_1(\mathbf{k})$, and $E_4(\mathbf{k}) = -E_2(\mathbf{k})$. Here, the auxiliary energies are $\epsilon_1(\mathbf{k}) = \xi(\mathbf{k}) + h_\perp(\mathbf{k})$, and $\epsilon_2(\mathbf{k}) = \xi(\mathbf{k}) - h_\perp(\mathbf{k})$. The corresponding order parameter equations at the saddle point level is

$$\frac{V}{g} = \frac{1}{2} \sum_{\mathbf{k}} \left[\frac{X_1(\mathbf{k})}{2E_1(\mathbf{k})} + \frac{X_2(\mathbf{k})}{2E_2(\mathbf{k})} \right], \quad (9)$$

where $X_m(\mathbf{k}) = \tanh[E_m(\mathbf{k})/2T]$ ($m = 1, 2$). Since the mixture of equal mass fermions is balanced, the chemical potentials are the same $\mu_\uparrow = \mu_\downarrow = \mu$, and the associated number equation is $N = -\partial\Omega/\partial\mu$ that reduces to

$$N = \sum_{\mathbf{k}} \left[1 - \frac{X_1(\mathbf{k})}{2E_1(\mathbf{k})} \varepsilon_1(\mathbf{k}) - \frac{X_2(\mathbf{k})}{2E_2(\mathbf{k})} \varepsilon_2(\mathbf{k}) \right]. \quad (10)$$

In Fig. 1, we show the zero temperature behavior of $|\Delta_0|$ and μ as a function of $1/(k_F a_s)$ for various values of spin-orbit coupling in the equal-Rashba-Dresselhaus (ERD) and for Rashba-only (RO) cases. In the ERD case the order parameter $|\Delta_0|$ is independent of v , and the chemical potential $\mu(v)$ is simply $\mu(v) = \mu(0) - mv^2/2$, since the transverse field $h_\perp(\mathbf{k}) = v|k_x|$ can be eliminated by momentum shifts along the x -direction, effectively gauging away spin-orbit effects in the *charge or momentum* sector. This symmetry also implies that the critical temperature T_c as a function of $1/(k_F a_s)$ for finite v is the same as that for $v = 0$. However, in the RO case, shifts in momentum can not gauge away the spin-orbit coupling, and $|\Delta_0|$ increases with increasing v_R , while μ decreases as v_R increases, exhibiting the same tendency as in the ERD case. In the BCS regime, the increase of $|\Delta_0|$ with v_R also leads to an increase of T_c with increasing v_R .

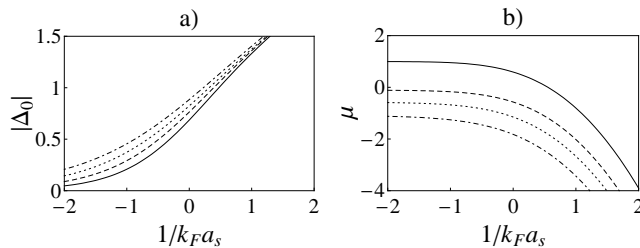


FIG. 1: Order parameter $|\Delta_0|$ and chemical potential μ (in units of the Fermi energy ϵ_F) as a function of interaction parameter $1/(k_F a_s)$ for different spin-orbit couplings $v_R/v_F = 0$ (solid), $v_R/v_F = 0.8$ (dashed), $v_R/v_F = 1.0$ (dotted), and $v_R/v_F = 1.2$ (dot-dashed) at $T = 0$ in the RO case. Here $v_F = k_F/m$ is the Fermi velocity.

Momentum distribution and excitation spectrum: The momentum distribution $n(\mathbf{k})$ is obtained from Eq. (10) using the definition $N = \sum_{\mathbf{k}} n(\mathbf{k})$. At fixed momentum component $k_z = 0$ and fixed interaction strength, the momentum distribution $n(\mathbf{k})$ shifts continuously with increasing spin-orbit coupling in the BCS [$1/(k_F a_s) \ll -1$] or unitarity regimes [$1/(k_F a_s) \rightarrow 0$]. For zero spin-orbit coupling, $n(\mathbf{k})$ is that of a superfluid degenerate Fermi system with identical single-particle bands $\xi(\mathbf{k})$ and has a nearly flat momentum distribution until the Fermi momentum is reached. However, as the spin-orbit coupling is turned on, non-identical single-particle bands $\xi_\uparrow(\mathbf{k}) = \xi(\mathbf{k}) - h_\perp(\mathbf{k})$ and $\xi_\downarrow(\mathbf{k}) = \xi(\mathbf{k}) + h_\perp(\mathbf{k})$ in the helicity basis $|\uparrow\rangle, |\downarrow\rangle$ emerge and produce a double

structure with a reasonably flat momentum distribution centered around finite momenta in the (k_x, k_y) plane. In the BEC regime [$1/(k_F a_s) \gg 1$] the momentum distributions for weak and strong spin-orbit coupling broadens substantially due to the loss of degeneracy in the Fermi system when the chemical potential goes below the minima of the helicity bands and becomes large and negative. Even though there is a substantial change in the momentum distribution as a function of the spin-orbit coupling, we notice that the excitation energies $E_1(\mathbf{k})$ and $E_2(\mathbf{k})$ is always gapped for all values of the interaction parameter $1/(k_F a_s)$ or the spin-orbit field $h_\perp(\mathbf{k})$, immediately suggesting that thermodynamic properties, which depend on the excitation energies, evolve smoothly from the BCS to the BEC regime in the balanced case for fixed values of spin-orbit coupling. The omnipresence of a gap in the excitation spectrum shows that the evolution from BCS to BEC superfluidity at finite spin-orbit coupling for balanced systems is just a crossover. The situation is different for imbalanced systems, where gapless regions emerge in the excitation spectrum and topological phase transitions occur, so long as the system is stable [9, 10]. A thermodynamic signature of this crossover for balanced systems is seen in the isothermal compressibility discussed next.

Isothermal compressibility: An important thermodynamic property, which can now be measured experimentally using the fluctuation-dissipation theorem, is the isothermal compressibility

$$\kappa_T = -\frac{1}{V} \left(\frac{\partial P}{\partial V} \right)_T = \frac{V}{N^2} \left(\frac{\partial N}{\partial \mu} \right)_T. \quad (11)$$

As shown in Fig. 2a, for the RO case, the isothermal compressibility κ_T at fixed interaction parameter $1/(k_F a_s)$ increases with increasing spin-orbit coupling v_R , as the Fermi system becomes less degenerate reducing the Pauli pressure, and thus more compressible. However, in the ERD case, the isothermal compressibility for fixed interaction parameter does not change with increasing spin-orbit coupling v . In this high symmetry situation the momentum shift in the energy spectrum and the accompanied shift in the chemical potential do not affect the degeneracy of the Fermi system or the Pauli pressure, leading to an isothermal compressibility which is independent of the spin-orbit coupling v .

Equation of State and Entropy: Since the thermodynamic potential $\Omega = -PV$, the saddle point pressure is $P_0(T, \mu_\alpha) = -\Omega_0/V$, which can be shown to be always positive for arbitrary spin-orbit coupling. The general trend of the pressure for fixed interaction parameter (from the BCS to the unitarity regimes) is to decrease with increasing spin-orbit coupling for both ERD and RO cases. The situation in the BEC regime requires the inclusion of quantum fluctuations to recover the corresponding Lee-Yang corrections in the presence of spin-orbit effects. The entropy is then calculated from

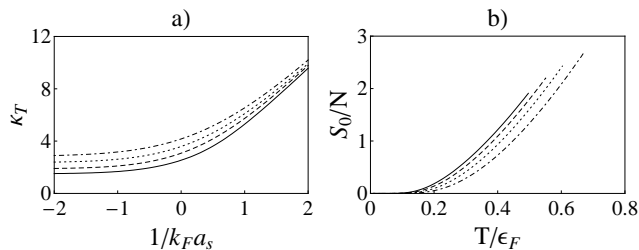


FIG. 2: a) Compressibility κ_T (in units of $1/(n\epsilon_F)$) as a function of interaction parameter $1/(k_F a_s)$ at $T = 0$ and b) entropy per particle S_0/N as a function of temperature T (in units of ϵ_F) at unitarity in the RO case, for the same group of spin-orbit coupling values v_R/v_F as in Fig. 1.

$S = -(\partial\Omega/\partial T)_{V,\mu_\alpha}$. In Fig. 2b, we show the saddle point entropy S_0 for the RO case at unitarity. For fixed T , S_0 decreases with increasing spin-orbit coupling due to the stabilization of superfluidity by the spin-orbit field.

Spin Susceptibility Tensor: A rotation of the matrix \mathbf{H}_0 into the helicity basis $|\uparrow\rangle, |\downarrow\rangle$ introduces order parameters $\Delta_{0,\uparrow\uparrow}$ and $\Delta_{0,\downarrow\downarrow}$, which are controlled by the spin-orbit coupling. The emergence of the triplet component affects dramatically the spin susceptibility of the system. Using standard linear response theory [11], the uniform spin susceptibility tensor per unit volume is

$$\chi_{ij} = -\frac{\mu_B^2}{V} \sum_{\mathbf{k}} [a_{ij}(\mathbf{k}) - b_{ij}(\mathbf{k})], \quad (12)$$

where the spin-spin correlations in the single-particle channel are $a_{ij}(\mathbf{k}) = \sum_{i\omega} \text{Tr} [\sigma_i \mathbf{G}(\mathbf{k}, i\omega) \sigma_j \mathbf{G}(\mathbf{k}, i\omega)]$ and in the pair (anomalous) channel are $b_{ij}(\mathbf{k}) = \sum_{i\omega} \text{Tr} [\sigma_i \mathbf{F}(\mathbf{k}, i\omega) \sigma_j^T \mathbf{F}^\dagger(\mathbf{k}, i\omega)]$. The matrices \mathbf{G} and \mathbf{F} are the block matrices appearing in the inverse of \mathbf{M} defined in Eq. (4),

$$\widetilde{\mathbf{M}}^{-1}(\mathbf{k}, i\omega) = \begin{pmatrix} \mathbf{G} & \mathbf{F} \\ \mathbf{F}^\dagger & \mathbf{G} \end{pmatrix}.$$

In Fig. 3a, we show plots of χ_{zz} for the ERD case at $T = 0$ as a function of $1/(k_F a_s)$ for various values of spin-orbit coupling, and the behavior of χ_{zz} for the RO case is qualitatively similar. In Fig. 3b, we show χ_{zz} versus v in the unitary limit $1/(k_F a_s) = 0$. The maximum in χ_{zz} corresponds to the maximum in the triplet component of Δ_0 . For small and large v the triplet component is small.

In the ERD case $\chi_{zz} = \chi_{xx} \neq \chi_{yy}$, and in the zero temperature limit $\chi_{yy}(T \rightarrow 0) = 0$, while $\chi_{zz} = \chi_{xx}$ remains finite for non-zero spin-orbit coupling. In the RO case $\chi_{zz} \neq \chi_{xx} = \chi_{yy}$, and in the $T \rightarrow 0$ limit $\chi_{xx}(T \rightarrow 0) = \chi_{yy}(T \rightarrow 0) = \chi_{zz}(T \rightarrow 0)/2$. Lastly, for $h_\perp(\mathbf{k}) = 0$ (no spin-orbit coupling) the spin susceptibility tensor becomes $\chi_{ij} = \chi \delta_{ij}$, where the scalar $\chi = [\mu_B^2/(2VT)] \sum_{\mathbf{k}} \text{sech}^2 \left[\sqrt{\xi_{\mathbf{k}}^2 + |\Delta_0|^2}/(2T) \right]$ is the Yoshida function, which vanishes at zero temperature,

i.e., $\chi(T \rightarrow 0) = 0$. The existence of non-zero spin response even at $T = 0$ is a direct measure of the induced triplet component of the order parameter due to the presence of spin-orbit coupling, since that a pure singlet superfluid at $T = 0$ must have zero spin susceptibility since all fermions are paired into a zero-spin state.

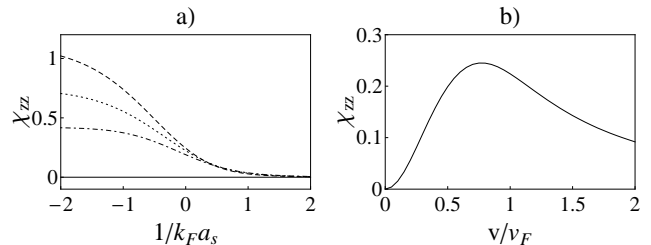


FIG. 3: a) Spin susceptibility χ_{zz} (in units of $\mu_B^2 n/\epsilon_F$) as a function of $1/(k_F a_s)$ at $T = 0$ in the ERD case for $v/v_F = 0$ (solid), $v/v_F = 0.8$ (dashed), $v/v_F = 1$ (dotted), and $v/v_F = 1.2$ (dot-dashed). b) Spin susceptibility χ_{zz} as a function of v/v_F at $T = 0$ at unitarity in the ERD case.

Conclusions: We have studied the effects of spin-orbit coupling in the evolution from BCS to BEC superfluidity at low temperatures, and concluded that this evolution is just a crossover. We discussed effects of spin-orbit coupling on thermodynamic properties including the order parameter, chemical potential, pressure, entropy, isothermal compressibility and spin susceptibility tensor to support the crossover picture. We also proposed way to experimentally detect the spin-orbit coupling effect by measuring the spin susceptibility.

We would like to thank NSF (Grant No. DMR-0709584) and ARO (Contract No. W911NF-09-1-0220).

-
- [1] Y. J. Lin, R. L. Compton, K. Jimenez-Garcia, J. V. Porto, and I. B. Spielman, *Nature (London)* **462**, 628 (2009).
 - [2] I. B. Spielman, *Phys. Rev. A* **79**, 063613 (2009).
 - [3] Y. J. Lin, K. Jimenez-Garcia, and I. B. Spielman, *Nature* **471**, 83 (2011).
 - [4] M. Chapman and C. Sá de Melo *Nature* **471**, 41 (2011).
 - [5] M. Iskin and C. A. R. Sá de Melo, *Phys. Rev. A* **83**, 045602 (2011).
 - [6] J. Dalibard, F. Gerbier, G. Juzeliūnas, P. Öhberg, *arXiv:1008.5378v1* (2010).
 - [7] G. Dresselhaus, *Phys. Rev.* **100**, 580 (1955).
 - [8] Y. A. Bychkov and E. I. Rashba, *J. Phys. C* **17**, 6029 (1984).
 - [9] M. Iskin and C. A. R. Sá de Melo, *Phys. Rev. Lett.* **97**, 100404 (2006).
 - [10] M. Gong, S. Tewari, C. Zhang, *arXiv:1105.1796v1* (2011).
 - [11] Lev P. Gor'kov and E. I. Rashba, *Phys. Rev. Lett.* **87**, 037004 (2001).